Ad Hoc Networks 37 (2016) 183–194

Contents lists available at ScienceDirect

Ad Hoc Networks

journal homepage: www.elsevier.com/locate/adhoc

On power control in full duplex underlay cognitive radio networks☆

Ningkai Tang[a], Shiwen Mao[a,*], Sastry Kompella[b]

[a] Department of Electrical and Computer Engineering, Auburn University, Auburn, AL, USA
[b] Information Technology Division, Naval Research Laboratory, Washington, DC, USA

ARTICLE INFO

Article history:
Received 29 November 2014
Revised 24 May 2015
Accepted 27 August 2015
Available online 7 September 2015

Keywords:
Cognitive radio
Control theory
Full duplex transmission
Interference mitigation
Power control
Stability

ABSTRACT

Both cognitive radio (CR) and full duplex transmissions are effective means to enhance spectrum efficiency and network capacity. In this paper, we investigate the problem of power control in an underlay CR network where the CR nodes are capable of full-duplex (FD) transmissions. The objective is to guarantee the required quality of service (QoS) in the form of a minimum signal-to-interference-plus-noise (SINR) ratio at each CR user and keep the interference to primary users below a prescribed threshold. We design an effective distributed power control scheme that integrates a proportional-integral-derivative (PID) controller and a power constraint mechanism to achieve the above goals. We analyze the stability performance of the proposed scheme and develop a hybrid scheme that can switch between FD and half duplex (HD) modes. The proposed scheme is validated with extensive simulations.

1. Introduction

In recent years, an unprecedented increase in wireless data has been observed. This is largely due to the proliferation of smartphones, tablets and other wireless devices, each generating tens or hundreds times of wireless data than a traditional mobile phone [2]. The exploding wireless data calls for effective technologies for enhancing spectrum utilization and wireless network capacity. To this end, cognitive radios (CR) have been recognized as one of the key technologies to meet this grand challenge on wireless network capacity. As an effective means of sharing spectrum among licensed (i.e., primary) users (PU) and unlicensed (i.e., secondary) users (SU), CR has been demonstrated to achieve high utilization of the scarce spectrum resource [3,4].

In CR networks, the most important design factor is to balance the tension between PU protection and SU spectrum access gains [3]. On one hand, the capacity of SUs should be maximized to "squeeze" the most out of the spectrum. On the other hand, the adverse impact to PUs, resulting from sharing spectrum with SUs, should be kept below a tolerable level. Obviously, these are two conflicting goals that should be balanced in the design of CR networks. In the so-called overlay CR networks, PU protection is achieved by spectrum sensing and spectrum access only when the PUs are sensed absent [3]. In the so-called underlay CR networks, both PU and SU transmissions coexist in the same spectrum band, and PU protection is achieved by carefully controlling the power of the SU transmitters [5].

Recently, a breakthrough in wireless communications is full duplex (FD) transmissions [6–9]. Traditionally, wireless communications are all half duplex (HD) due to the large path loss typical in wireless transmissions. If FD transmission is allowed, the self-interference will be so strong (like the sun) and the weak received signal from a remote transmitter (like stars) will be completely overwhelmed and cannot be

☆ This paper was presented in part at IEEE MILCOM 2014, Baltimore, MD, USA, Oct. 2014 [1].

* Corresponding author. Tel.: +1 334 844 1845; fax: +1 334 844 1809.
E-mail addresses: nzt0007@tigermail.auburn.edu (N. Tang), smao@ieee.org (S. Mao), sk@ieee.org (S. Kompella).

http://dx.doi.org/10.1016/j.adhoc.2015.08.018
1570-8705/

decoded. Recently, encouraging results have been reported on enabling FD wireless transmissions in both single link and a network setting [6–9]. The enabler of FD is the recent advances in self-interference suppression (SIS). Various effective SIS techniques have been proposed and tested, such as antenna separation [6], antenna cancellation [7], signal inversion and adaptive cancellation [8], and combined optimal antenna placement and analog cancellation [10]. In [10], the authors presented a practical implementation that can suppress self-interference (SI) for up to 80 dB, which should be sufficient for many application environments [11]. The achievable capacity gain of FD in a network setting is investigated in a few recently works [12–14], where inter-link interference and spatial reuse are the major limiting factors for the FD gain [13].

In a recent work [11], the authors propose to integrate FD in overlay CR networks. It is demonstrated that an FD-enabled SU can operate in either simultaneous transmit-and-sense mode or simultaneous transmit-and-receive mode. The authors analytically study the performance of the two modes and evaluate the sensing-throughput tradeoff for both modes. Motivated by this work, in this paper, we investigate the problem of integrating FD in underlay CR networks. We consider a primary network co-located with multiple SU links. The SUs are capable of FD transmissions. As discussed, the key design issue for underlay CR networks is how to design an effective power control scheme to achieve the dual goal of PU protection and SU spectrum access gain maximization.

For PU protection, we consider multiple detection points (DP) in the network for measuring interference from SU transmissions. Such DPs can be special devices deployed at strategic locations, such as base stations in primary networks [18]. The PUs incorporate a short Quiet Period in each time frame as in IEEE 802.22 Wireless Regional Area Networks (WRAN) [15], during which the PUs stop their transmissions and the DPs can measure the interference from SU transmissions together with other noise to set the noise floor for SUs. Based on the noise floor set by DPs, each SU transmitter adjusts its transmit power to achieve the primary goal of keeping the measured interference to PUs below a prescribed threshold, and the secondary goal of guaranteeing the quality of service (QoS) of SUs in the form of a minimum signal-to-interference-plus-noise ratio (SINR).

We develop a distributed power control scheme that consists of a proportional-integral-derivative (PID) controller, for satisfying the SU QoS requirements, and an additional power constraint mechanism, for PU protection. We analyze the stability of the proposed power control scheme and develop a hybrid HD–FD scheme for harvesting the benefits of both modes under various network and system settings. The proposed schemes are evaluated with extensive simulation studies.

In the remainder of this paper, we first present the system model and problem statement in Section 2. In Section 3 we develop the power control scheme and in Section 4 we analyze its stability performance and develop a hybrid HD/FD scheme. Simulation results are presented in Section 5 and related work discussed in Section 6. Section 7 concludes the paper.

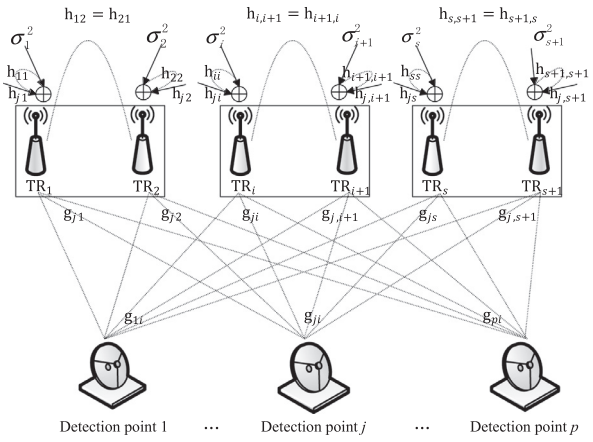

Fig. 1. An FD underlay CR network considered in this paper.

2. System model and problem statement

2.1. System model

Consider an underlay CR network as illustrated in Fig. 1. There is a primary network with active transmissions using a licensed spectrum band. A co-located secondary network consists of $(s+1)$ SUs, termed TR_i, $i = 1, 2, \ldots, s+1$, where s is an odd number. The SUs are paired to form $(s+1)/2$ FD transmission links, i.e., TR_i is transmitting to, and simultaneously receiving from TR_{i+1}, while i is an odd index. Due to the underlay spectrum sharing policy, the SUs are allowed to use the same spectrum band as the primary network. For protection of the primary network, there are p detection points (DP) in the primary work that measure the interference from the secondary transmissions during the Quiet Periods [15]. As discussed, such DPs can be standalone devices deployed in strategic locations in the network area, or simply a piece of program running in the primary receivers or SUs. The measured SU interference should be kept below a threshold at the DP locations by effectively controlling the power of the secondary transmitters.

Note that the DPs are an important part of the network architecture considered in this paper. In fact, although in the earlier stage, especially in dynamic spectrum access (DSA), it was desirable to make spectrum sharing unobtrusive to PUs [4], the great benefits and need of participation/cooperation of PUs in spectrum sharing has been recognized in recent works [16,17]. This is particularly true in underlay CR networks, where CR users can access the spectrum freely as long as the interference PUs receive is below a threshold. In such networks, CR users need to know the interference level at primary users, which is extremely challenging (or impossible) without deploying some measurement mechanisms or involvement of PUs.

To address this problem, there has been proposals on deploying spectrum sensors in the CR network [18,19], i.e., "use a large number of sensors to properly 'sniff' the RF environment, wherever it is feasible. The large number of sensors is needed to account for the spatial variation of the RF stimuli from one location to another" [18]. This is actually

the approach adopted in this paper. Another approach in the literature involves PUs in the process [24]. To satisfy the interference constraint at the PUs, channel state information (CSI) is needed for channels between SU transmitters and receivers, and the channels between SU transmitter and PU receivers [20–23]. When the CSI and the SU transmit powers are known, the SU interference at PUs can be computed. The CSI can be fedback directly by the PUs, measured by SUs (assuming channel reciprocity), or through a centralized controller that manages spectrum sharing [20]. This is the case when the DPs are actually an agent running in the PUs to feedback CSI to the SUs, and the interference $y_i(t)$ at PU i (or, DP i) is actually calculated. Of course, the DP agents in the PUs can feedback measured interference at the PUs instead of CSI. Then this is exactly the model adopted in this paper.

In Fig. 1, g_{ij} denotes the channel gain from TR_i to DP_j; h_{ij} represents the channel gain from TR_i to TR_j; and σ_i^2 is the sum of the total interference from primary transmissions and the noise power at TR_i. To simplify notation, we assume channel reciprocity, i.e., h_{ij} (or g_{ij}) is equal to h_{ji} (or g_{ji}) for all i, j. For each FD link, the self-interference is $P_i(t)h_{ii}^2$, where $P_i(t)$ is the transmit power of TR_i and h_{ii} is the channel gain from TR_i's transmitting antenna to the receiving antenna. We assume that each TR_i utilizes SIS, and the residual self-interference is reduced to $\chi P_i(t)h_{ii}^2$, where χ is a constant in [0, 1] depending on the specific SIS design. When $\chi = 0$, it is the ideal case where the self-interference can be completely canceled; when $\chi = 1$, it is the worst case without SIS and FD transmission is not possible. Usually χ is a small number, e.g., at least 45dB across a 40 MHz band and up to 73dB for a 10 MHz OFDM signal [8].

2.2. Problem statement

For the FD CR network to work properly, two conditions should be satisfied by controlling the transmit power of the TR_j's. The first condition is *primary user protection*. That is, the measured interference from secondary transmissions should be kept below a prescribed tolerance level D_j at each DP_j. The second condition is *guaranteeing the QoS of SUs*. That is, the SINR at the TR_i's should be kept above a prescribed threshold Γ, such that the SUs can be guaranteed with a minimum data rate.

We assume that time is slotted. To achieve these goals, in each time slot t, a centralized power control algorithm updates the transmit power of each TR_i, denoted as $P_i(t)$, according to the measured radio environment, as

$$P_i(t+1) = P_i(t) + u_i(t), \tag{1}$$

where $u_i(t)$ is the increment (positive or negative) of power at TR_i in time slot t.

As shown in Fig. 1, the total interference from the TRs to a detection point DP_j is

$$y_j(t) = \sum_{k=1}^{s+1} P_k(t)g_{kj}^2, \quad j = 1, 2, \ldots, p. \tag{2}$$

Then the primary user protection constraint becomes

$$y_j(t) \le D_j, \quad j = 1, 2, \ldots, p. \tag{3}$$

For time slot $t+1$, the secondary interference $y_j(t+1)$ caused by the updated transmit powers should also satisfy (3), i.e.,

$$y_j(t+1) \le D_j, \quad j = 1, 2, \ldots, p. \tag{4}$$

For the second constraint on guaranteeing the QoS of SUs, the SINR at the receiving antenna of TR_i can be written as

$$\gamma_i(t) = \begin{cases} \dfrac{P_{i+1}(t)h_{i+1,i}^2}{\sum_{j=1,j\neq i}^{s+1} P_j(t)h_{ji}^2 + \chi_i P_i(t)h_{ii}^2 + \sigma_i^2(t)}, & i \text{ is odd} \\ \dfrac{P_{i-1}(t)h_{i-1,i}^2}{\sum_{j=1,j\neq i}^{s+1} P_j(t)h_{ji}^2 + \chi_i P_i(t)h_{ii}^2 + \sigma_i^2(t)}, & i \text{ is even,} \end{cases} \tag{5}$$

where χ_j is the SIS factor [11]. Recall that $u_i(t) = P_i(t+1) - P_i(t)$. From the control point of view, (5) can be regarded as the state equation and $u_i(t)$ the input. The updated state is

$$\gamma_i(t+1) = \begin{cases} \gamma_i(t) + \dfrac{h_{i+1,i}^2}{I_i(t)}u_i(t) \\ \quad + \dfrac{P_i(t+1)h_{i+1,i}^2[I_i(t) - I_i(t+1)]}{I_i(t)I_i(t+1)}, & i \text{ is odd} \\ \gamma_i(t) + \dfrac{h_{i-1,i}^2}{I_i(t)}u_i(t) \\ \quad + \dfrac{P_i(t+1)h_{i-1,i}^2[I_i(t) - I_i(t+1)]}{I_i(t)I_i(t+1)}, & i \text{ is even,} \end{cases} \tag{6}$$

where

$$I_i(t) = \sum_{j=1,j\neq i}^{s+1} P_j(t)h_{ji}^2 + \chi_i P_i(t)h_{ii}^2 + \sigma_i^2(t). \tag{7}$$

It is shown that generally $I_i(t) - I_i(t+1)$ is much smaller than $I_i(t)I_i(t+1)$ [25]. It follows that (6) can be approximated as

$$\gamma_i(t+1) = \begin{cases} \gamma_i(t) + \dfrac{h_{i,i+1}^2}{I_i(t)}u_i(t), & i \text{ is odd} \\ \gamma_i(t) + \dfrac{h_{i,i-1}^2}{I_i(t)}u_i(t), & i \text{ is even.} \end{cases} \tag{8}$$

Let Γ denote the minimum required SINR for SU TR_i. The SU QoS constraint is

$$\gamma_i(t) \ge \Gamma. \tag{9}$$

The updated $\gamma_i(t+1)$ should also satisfy condition (9), i.e.,

$$\gamma_i(t+1) \ge \Gamma. \tag{10}$$

2.3. Centralized scheme

Assuming global information about the channels, transmit powers and measured interference, the power increments can be solved in a centralized manner. Define parameters a and b as

$$a = \begin{cases} [u_i(t) + P_i(t)]h_{i+1,i}^2, & i \text{ is odd} \\ [u_i(t) + P_i(t)]h_{i-1,i}^2, & i \text{ is even.} \end{cases} \tag{11}$$

$$b = \sum_{j=1, j\neq i}^{s+1} [u_j(t) + P_j(t)]h_{ji}^2 + \chi_i[u_i(t) + P_i(t)]h_{ii}^2 + \sigma_i^2(t+1), i = 1, 2, \ldots, s+1. \quad (12)$$

From (1), (4), and (10), we derive the following system of equations that can be solved for $u_i(t)$.

$$\begin{cases} a/b = \Gamma, \ i = 1, 2, \ldots, s+1 \\ [u_i(t) + P_i(t)]g_{ij}^2 + \sum_{k=1, k\neq i}^{s+1} [u_k(t) + P_k(t)]g_{kj}^2 \leq D_j, \ j = 1, 2, \ldots, p. \end{cases} \quad (13)$$

If the channel gains vary over time (e.g., in a mobile SU network), we can defined parameters a^* and b^* as

$$a^* = \begin{cases} [u_i(t) + P_i(t)]h_{i+1,i}^2(t+1), i \text{ is odd}, \\ [u_i(t) + P_i(t)]h_{i-1,i}^2(t+1), i \text{ is even}. \end{cases} \quad (14)$$

$$b^* = \sum_{j=1, j\neq i}^{s+1} [u_j(t) + P_j(t)]h_{ji}(t+1)^2 + \chi_i[u_i(t) + P_i(t)]h_{ii}(t+1)^2 + \sigma_i^2(t+1), i = 1, \ldots, s+1. \quad (15)$$

A similar system of equations can be solved to determine $u_i(t)$ as

$$\begin{cases} a^*/b^* = \Gamma, i = 1, 2, \ldots, s+1 \\ [u_i(t) + P_i(t)]g_{ij}^2(t+1) + \sum_{k=1, k\neq i}^{s+1} [u_k(t) + P_k(t)]g_{kj}^2(t+1) \leq D_j, \ j = 1, 2, \ldots, p. \end{cases} \quad (16)$$

3. Distributed power control

In this section, we develop a power control scheme for adapting the transmit power of the secondary users [26]. The goal is to achieve the SU QoS requirement while satisfying PU protection constraint as given in (13). The proposed scheme is a distributed algorithm in the sense that each TR_i adjusts its power P_i independently. However, each TR_i needs to know the minimum tolerable interference level and the maximum measured SU interference at all the DPs.

3.1. A PID controller

First, we consider the SU QoS constraint, while ignoring the PU protection constraint. The goal is to drive $\gamma_i(t)$ to converge to the SU QoS requirement Γ, for all i. The difference between these two parameters should be considered and should be reduced to as small as possible. Another consideration is that the error signal $e_i(t)$ should be related to the power $P_i(t)$, which is the parameter that we need to determine for each TR_i. Therefore $P_i(t)$ is used as the reference input. As we can see, the ratio of Γ and $\gamma_i(t)$ can be an indicator for the control error, and $\gamma_i(t) \propto P_i(t)$ if all other parameters remain the same. Thus, we use $\frac{\Gamma}{\gamma_i(t)}P_i(t)$ as the feedback. The error $e_i(t)$ should be the difference of feedback and $P_i(t)$ and we have the diagram of the PID controller as in Fig. 2.

The PID controller collects the SINR of each TR at every time slot and uses it as feedback for the controller. For each time slot, let $z_i(t)$ denote the power increment from $P_i(t)$ to $P_i(t+1)$. With feedback $\frac{\Gamma}{\gamma_i(t)}P_i(t)$, the PID controller controls the system as

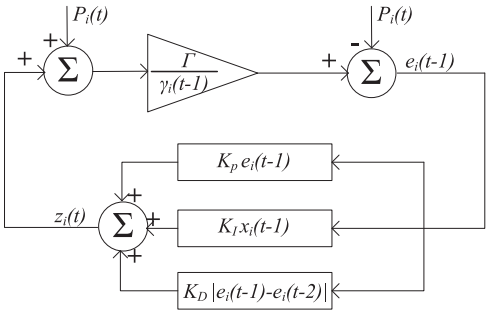

Fig. 2. The PID controller design.

$$e_i(t-1) = \left\{ \frac{\Gamma}{\gamma_i(t-1)} - 1 \right\} P_i(t) \quad (17)$$

$$x_i(t-1) = x_i(t-2) + e_i(t-1) \quad (18)$$

$$z_i(t) = K_P e_i(t-1) + K_I x_i(t-1) + K_D \left| e_i(t-1) - e_i(t-2) \right|, \quad (19)$$

where $e_i(t-1)$, $x_i(t-1)$ and $\left|e_i(t-1) - e_i(t-2)\right|$ represent the proportional, integral and derivative parts, respectively; K_p, K_I, and K_D are the corresponding coefficients. Proper coefficients should be designed to achieve a stable and convergent control process for adjusting the $P_i(t)$'s to achieve the required minimum SINR Γ for each SU [27].

3.2. Power control constraint

Next we take into account the PU protection constraint. The objective of this constraint is to prevent the SU transmission powers from violating the interference tolerance at the DPs. This constraint actually represents a relationship between $P_i(t)$ and D_j, for all i and j.

We first introduce the following two parameters.

$$D_{min} = \min_{j=1,2,\ldots,p} D_j \quad (20)$$

$$y_{max}(t-1) = \max_{j=1,2,\ldots,p} y_j(t-1). \quad (21)$$

D_{min} is the minimum tolerance value among all the DPs, and $y_{max}(t)$ is the maximum measured interference among all DPs. Since D_{min} is a constant and $y_{max}(t-1) \propto P_i(t-1)$, the additional power constraint should also be proportional to $P_i(t-1)$. We follow a similar approach as in prior work [5] to introduce the following additional constraint on the power adjustment $z_i(t)$.

$$c_i(t) = \theta(t)P_i(t-1) - P_i(t), \quad (22)$$

where,

$$\theta(t) = \frac{D_{min}}{y_{max}(t-1)}. \quad (23)$$

According to (22) and (23), once the maximum interference $y_{max}(t-1)$ exceeds the minimum tolerance D_{min}, the constraint will reduce the transmit power with a proportion

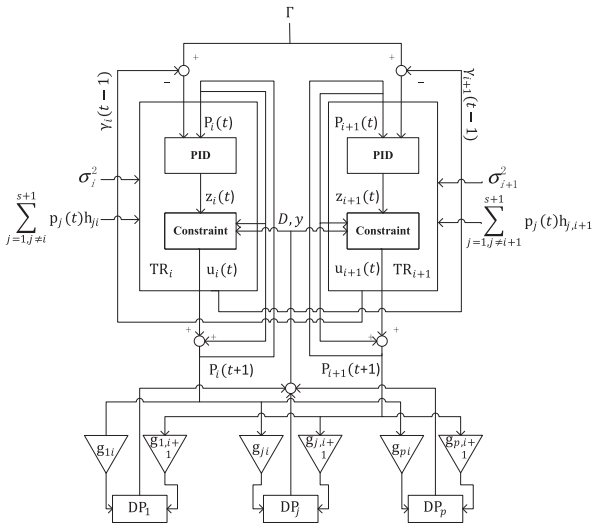

Fig. 3. System control block diagram.

of $\theta(t)$, which will drive the maximum interference back to the minimum tolerance D_{min}.

Eq. (22) enforces an additional constraint to the power increment $z_i(t)$ for the SUs, so as to satisfy the PU protection constraint as given in (3). Because the PU protection is a fundamental condition for spectrum sharing, the constraint $c_i(t)$ cannot be violated. Therefore, we have the final allowed power increment $u_i(t)$ in time slot t for TR_i as

$$u_i(t) = \min\{z_i(t), c_i(t)\},\ i = 1, 2, \ldots, s+1. \tag{24}$$

With such adjustment, the transmit power can be limited in a safe range that does not lead to severe interference to the primary network, while trying to achieve the minimum required SINR for the SUs. The overall diagram of the proposed power controller is illustrated in Fig. 3.

4. Performance analysis

4.1. Stability analysis

It is important to analyze the stability performance of the proposed power control scheme. The stability of the PID controller (i.e., without considering FD and the PU protection constraint (22)) can be analyzed as in [26]. The stability of the overall scheme depends on the parameter settings. In the following, we examine two cases when each of the two constraints, i.e., $z_i(t)$ and $c_i(t)$, becomes the dominant factor at the beginning stage.

4.1.1. Case I: $z_i(t) > c_i(t)$ Initially

From (17), (18) and (19), we have $P_i(0) = P_i(1) = P_i(2)$, and $x_i(0) = e_i(0) = 0$ for the initial time slots. There is no power adjustment in the first time slot, and the first power adjustment occurs at $t = 2$, as

$$z_i(2) = (K_P + K_I + K_D)e_i(1). \tag{25}$$

If $z_i(2) > c_i(2)$, from (24) we have $u_i(2) = c_i(2)$ and

$$\begin{cases} P_i(3) = \theta(2)P_i(1) \\ P_i(4) = \theta(3)P_i(2). \end{cases} \tag{26}$$

After the power adjustment in time slot 2, the detected total SU interference at DP j in time slot 3 is

$$\begin{aligned} y_j(3) &= \sum_{i=1}^{s+1} P_i(3)g_{ij}^2 = \sum_{i=1}^{s+1} \theta(2)P_i(1)g_{ij}^2 \\ &= \frac{D_{min}}{y_{max}(1)} \sum_{i=1}^{s+1} P_i(1)g_{ij}^2. \end{aligned}$$

The maximum measured interference among all the DPs is

$$\begin{aligned} y_{max}(3) &= \max_{j=1,\ldots,p} y_j(3) \\ &= \frac{D_{min}}{y_{max}(1)} \max_{j=1,\ldots,p} \sum_{i=1}^{s+1} P_i(1)g_{ij}^2 \\ &= \frac{D_{min}}{y_{max}(1)} y_{max}(1) = D_{min}. \end{aligned} \tag{27}$$

Therefore the maximum measured interference will remain at D_{min} and the constraint $c_i(t)$ will remain at 0 starting from time slot 3. According to (24), $u_i(t)$ will also remain at 0 after time slot 3. All the transmit powers converge to the steady value and the primary goal of PU protection is satisfied. However, there is no guarantee that the target SU QoS requirement can be achieved by the converged TR powers. If $\gamma_i(3) < \Gamma$, the SU QoS requirement cannot be satisfied since the transmit powers cannot be adjusted anymore.

If $z_i(t)$ remains non-negative, $u_i(t)$ will always be 0 since $c_i(t) = 0$ for all $t \geq 3$. All the TR powers will remain the same and the maximum measured interference remains at D_{min}. Otherwise, if $z_i(t) < 0$ due to some disturbance, the TR_i power will be reduced with $z_i(t)$, until the target SINR Γ is reached. However, if the above two situations both happens during the control process, we can predict that there will be oscillation and the system will enter a bounded oscillation state. Therefore, the system can be called bounded-in-bounded-out (BIBO) stable. In summary, for all the three cases discussed above, the system will be stabilized by the proposed power control scheme.

4.1.2. Case II: $z_i(t) < c_i(t)$ Initially

On the other hand, if the control function is initially dominated by the PID controller adjustment $z_i(t)$, the pattern changes. If the transmit powers to achieve the desired SINR cause a smaller measured interference than the D_j's, that is, if the primary network has high interference tolerance D_j's, the additional constrain enforced by $c_i(t)$ can be ignored, and the power control will become a stable PID control process. The stability of such a system has been demonstrated in [26].

However, if the desired SINR Γ cannot be achieved due to a small D_{min}, the PU protection constraint will take over the control during the process and will drive the TR powers to the maximum allowed value. The other situation is that due to the impact of some disturbance, the control process may enter the same BIBO state as discussed in Section 4.1.1.

4.2. Hybrid HD–FD operation

Recall that the SIS factor χ depends on the particular SIS design and is a small value in [0, 1]. Clearly, χ, along with

other network dynamics such as the channel gains, the number and locations of SUs and DPs, and the prescribed control goals (i.e., Γ and D_j's), all have big impact on the system performance. So in a practical underlay CR network, it is not true that FD transmissions will always achieve a better performance; when χ is large, the residual self-interference will be so large that HD transmissions will be a better choice [12–14]. Therefore, a hybrid scheme that can switch between FD and HD modes, depending on the system parameters and states, would be highly desirable. In the following, we investigate the condition under which a switching between HD and FD modes should be made.

We use Shannon's capacity to approximate the throughput of an SU, i.e., $C = B\log_2(1+SINR)$. Since bandwidth B is a constant for all SUs, we use the spectrum efficiency $\log_2(1+SINR)$ for comparing the efficiency of the two operation modes in the following. Let γ_i^{FD} and γ_i^{HD} denote the SINRs of TR_i in the FD mode and HD mode, respectively. We can derive the average throughput for the SU pair in the HD mode, denoted as R_i^{HD}, as follows.

$$R_i^{HD} = \begin{cases} \frac{1}{2}\left[\log_2(1+\gamma_i^{HD}) + \log_2(1+\gamma_{i+1}^{HD})\right], & i \text{ is odd} \\ \frac{1}{2}\left[\log_2(1+\gamma_i^{HD}) + \log_2(1+\gamma_{i-1}^{HD})\right], & i \text{ is even,} \end{cases} \tag{28}$$

where,

$$\gamma_i^{HD} = \begin{cases} \frac{P_{i+1}(t)h_{i+1,i}^2}{\sum_{j=1,j\neq i}^{s+1} P_j(t)h_{ji}^2 + \sigma_i^2(t)}, & i \text{ is odd} \\ \frac{P_{i-1}(t)h_{i-1,i}^2}{\sum_{j=1,j\neq i}^{s+1} P_j(t)h_{ji}^2 + \sigma_i^2(t)}, & i \text{ is even.} \end{cases} \tag{29}$$

In the FD mode, the throughput for the SU pair is

$$R_i^{FD} = \begin{cases} \log_2(1+\gamma_i^{FD}) + \log_2(1+\gamma_{i+1}^{FD}), & i \text{ is odd} \\ \log_2(1+\gamma_i^{FD}) + \log_2(1+\gamma_{i-1}^{FD}), & i \text{ is even,} \end{cases} \tag{30}$$

where γ_i^{FD} is given in (5).

In each time slot t, we estimate the expected throughput for each SU pair in both the FD and HD modes and decide which mode to adopt for the time slot. The cross-over point for the two modes is derived by solving the following equation.

$$R_i^{HD} = R_i^{FD}. \tag{31}$$

It can be seen that (31) can be rewritten as

$$\begin{cases} \sqrt{(1+\gamma_i^{HD})(1+\gamma_{i+1}^{HD})} = (1+\gamma_i^{FD})(1+\gamma_{i+1}^{FD}), \\ \quad i \text{ is odd} \\ \sqrt{(1+\gamma_i^{HD})(1+\gamma_{i-1}^{HD})} = (1+\gamma_i^{FD})(1+\gamma_{i-1}^{FD}), \\ \quad i \text{ is even.} \end{cases} \tag{32}$$

Define a ratio T_i as follows.

$$T_i = \begin{cases} \frac{\sqrt{(1+\gamma_i^{HD})(1+\gamma_{i+1}^{HD})}}{(1+\gamma_i^{FD})(1+\gamma_{i+1}^{FD})}, & i \text{ is odd} \\ \frac{\sqrt{(1+\gamma_i^{HD})(1+\gamma_{i-1}^{HD})}}{(1+\gamma_i^{FD})(1+\gamma_{i-1}^{FD})}, & i \text{ is even.} \end{cases} \tag{33}$$

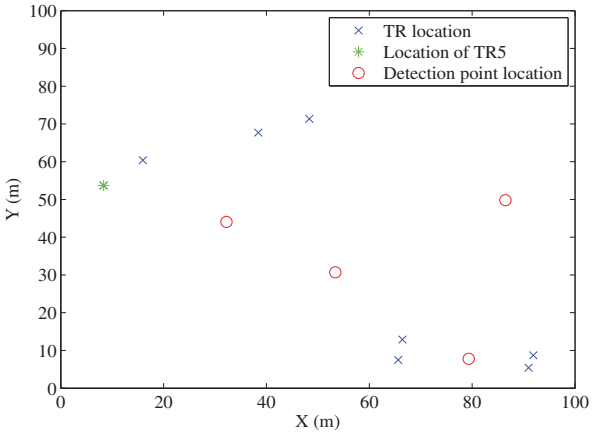

Fig. 4. Distribution of the TRs and DPs in the 100 × 100 m² network.

Thus, we have the following proposition for determining the operation mode for TR_i in the hybrid scheme.

Proposition 1. *TR_i should operate in the HD mode if $T_i \geq 1$, and it should operate in the FD model if $T_i < 1$.*

5. Simulation study

5.1. Simulation configuration

To evaluate the performance of the proposed power control scheme for FD underlay CR networks, we conduct extensive simulations using a MATLAB implementation. We use one network in a 100 × 100 m² area and another network in a 1000 × 1000 m² area. The outdoor channel model [28]

$$h = 40\log_{10}(d) + 30\log_{10}(f) + 49\text{dB}$$

is used in all the simulations, where d is the distance between the transmitter and receiver in kilometers and f set as 500 is the carrier frequency in MHz. In each simulation, the noises powers σ^2 are i.i.d. random variables evenly distributed in a fixed range, while the range may change in different simulations. As discussed, the performance of FD systems are greatly affected by χ. We choose $\chi = 10^{-7}$ in most of the simulations, unless otherwise specified.

There are eight TRs and four DPs in each of the networks. The location of the TRs and DPs are shown in Figs. 4 and 16. We assume the DPs can communicate with each other to obtain information about detected interference levels at the DPs (i.e., $y_j(t-1)$) and broadcast the maximum detected interference (i.e., $y_{max}(t-1)$) to all the TRs through a control channel. The control goals Γ and D_j's are prescribed and is known to all the TRs in advance. Such information is used as input to the control scheme executed at each TR to adjust its transmit power.

5.2. Controller performance

In this section, we evaluate the performance of the proposed controller in the FD and HD modes. First, we simulate the 100 × 100 m² network under fixed Γ and fixed χ. We set $\Gamma = 0.8$ and $\chi = 10^{-7}$ in the simulation. Noise σ^2 is uniform

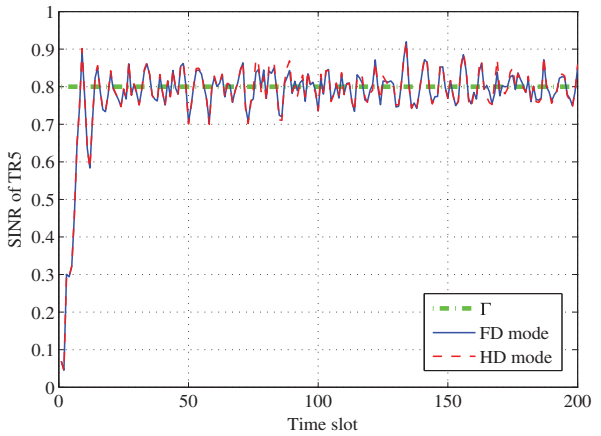

Fig. 5. Evolution of the SINR at TR_5 when $\Gamma = 0.8$ and $\chi = 10^{-7}$.

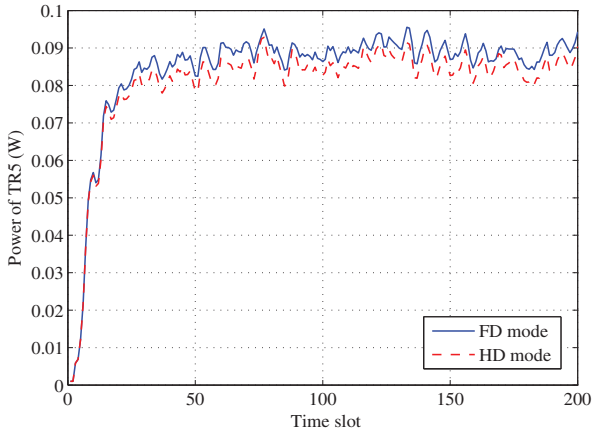

Fig. 6. Evolution of the transmit power at TR_5 when $\Gamma = 0.8$ and $\chi = 10^{-7}$.

distributed in $[1.2 \times 10^{-7}, 2.4 \times 10^{-7}]$ W. DP's tolerance limit is set as $D_j = 1 \times 10^{-7}$ W for all j.

Take TR_5 as an example. The evolutions of its SINR $\gamma_5(t)$ and transmit power $P_5(t)$ are plotted in Figs. 5 and 6, respectively. It can be seen that both the SINR and power curves quickly converge to the neighborhood of the stable values, and then fluctuate around the stable values. In Fig. 6, a higher transmit power is used in the FD mode to overcome the residual self-interference in order to achieve the target SINR value Γ.

In both cases, the control of the power adjustment is jointly done by both the PU protection constraint (22) and the SU QoS constraint (19). This can be witnessed by comparing $u_5(t) = \min\{z_5(t), c_5(t)\}$, $z_5(t)$, and $c_5(t)$ as plotted in Figs. 7, 8, and 9, respectively. In a few time slots the control process $u_5(t)$ reaches the stable value 0 and achieves the optimal SINR with the given D for TR_5.

In Fig. 10, we present the PU protection performance by plotting the PU interference tolerant D and the maximum measure interference $y_{max}(t)$ defined in (23) at the DPs for the FD and HD modes. It can be seen that with the proposed power control scheme, the maximum DP detected interference y_{max} is kept below D for all the time slots. Therefore the PU protection goal is well achieved by the proposed power

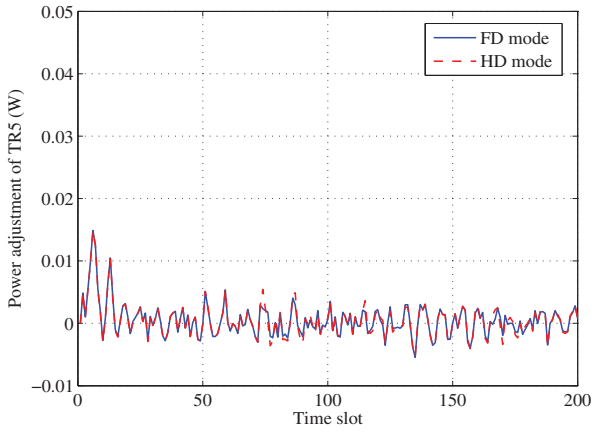

Fig. 7. Power adjustment $u_5(t) = \min\{z_5(t), c_5(t)\}$ of TR_5 when $\Gamma = 0.8$ and $\chi = 10^{-7}$.

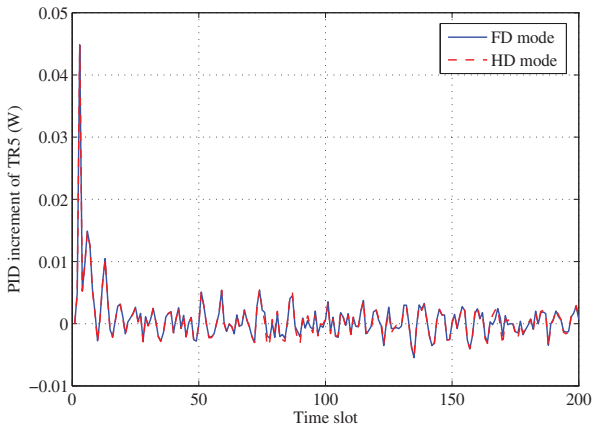

Fig. 8. PID controller adjustments $z_5(t)$ of TR_5 when $\Gamma = 0.8$ and $\chi = 10^{-7}$.

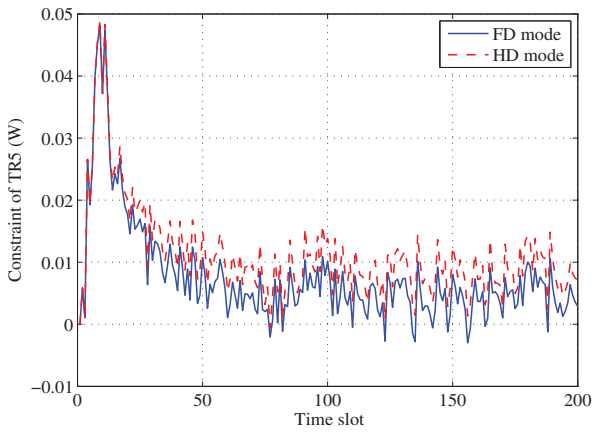

Fig. 9. PU protection constraint adjustments $c_5(t)$ of TR_5 when $\Gamma = 0.8$ and $\chi = 10^{-7}$.

control scheme. In the meantime, the controlled power remains around 0.09 W for the FD mode and 0.085 W for the HD mode (see Fig. 6), which are sufficient to satisfy the required SINR $\Gamma = 0.8$ for TR_5, as shown in Fig. 5. Since the controlled power of TR_5 has achieved both PU protection and SU

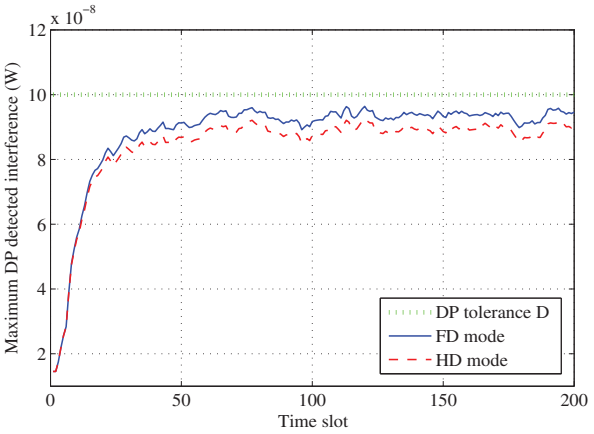

Fig. 10. Maximum measured interference among all the DPs when $\Gamma = 0.8$ and $\chi = 10^{-7}$.

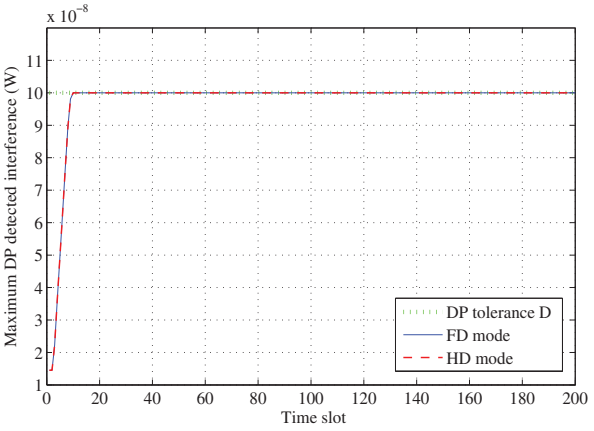

Fig. 11. Maximum measured interference among all the DPs when $\Gamma = 1.2$ and $\chi = 10^{-7}$.

QoS goals, the power adjustment $u_5(t)$ will stay within a narrow range around zero.

Next we try a large value of $\Gamma = 1.2$ in the simulation to evaluate the case of an overly high QoS requirement of the SUs that cannot be supported in the underlay CR network. That is, there is no feasible solution to satisfy both PU protection and SU QoS constraints in this case. In this case, the power control scheme will try to achieve PU protection as a primary goal, as the prerequisite condition for spectrum sharing, and then try to maximize the SINR of the SUs as a secondary goal. The maximum DP detected interferences to PUs are plotted in Fig. 11 for the FD and HD modes. The proposed power control scheme can effectively guarantee that the interference to PUs is below the tolerance D. The achieved SINR for TR5 is also plotted for the FD and HD modes in Fig. 12. It can be seen that the SINR of TR_5 is stabilized around 0.67 for both modes, although the desired SINR for TR_5 is 1.2. Since the maximum allowed interference has been reached (i.e., $D = 10^{-7}$ W as in Fig. 11), the power of TR_5 cannot be further increased to reach the target SINR level $\Gamma = 1.2$. In fact we deliberately included this result to show a case that the target SINR cannot be achieved, i.e., given the current network condition and power constraints, there is

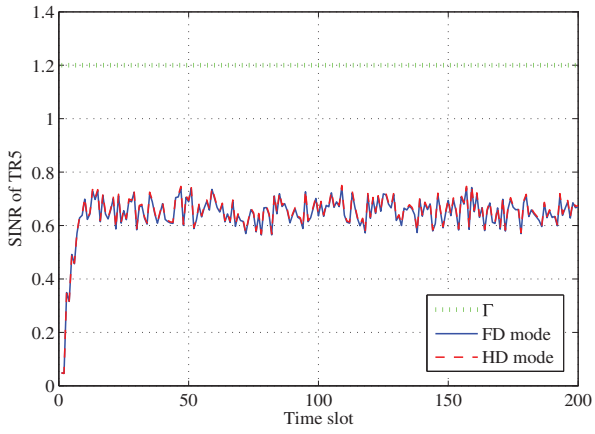

Fig. 12. Evolution of the SINR at TR_5 when $\Gamma = 1.2$ and $\chi = 10^{-7}$.

Table 1
Setting of Γ.

Time slot	1–50	51–100	101–150	151–200
Fig. 13	0.8	0.4	0.4	0.8
Figs. 14 & 15	0.4	0.8	1.2	1.6

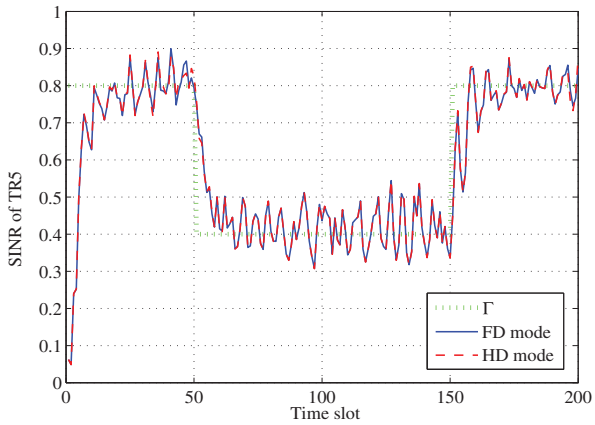

Fig. 13. Evolution of the SINR at TR_5 under varying Γ.

no feasible solution to the problem. This is true in the reality where resources are always limited and only certain design goals can be achieved. Therefore the SUs have to enjoy a lower throughput than expected. However, even in this case, the primary goal of protecting the PUs from harmful interference is still achieved. This actually demonstrates the design principle of cognitive radios, where the SUs aim to maximize their throughput without harming the PUs.

Finally, we demonstrate the performance of the proposed power controller under varying SU QoS requirements. In particular, we vary the SU SINR requirement Γ as given in Table 1. In Fig. 13, the required SINR is with the range such that the proposed controller can achieve both PU protection and SU QoS goals. It can be seen that the SINR can be stabilized around the target SINR for the full range. In Fig. 14, the SINR is continuously increased, from the feasible range to the infeasible range, where both goals cannot be met simultaneously. In Fig. 14, both SINR curves are well under control

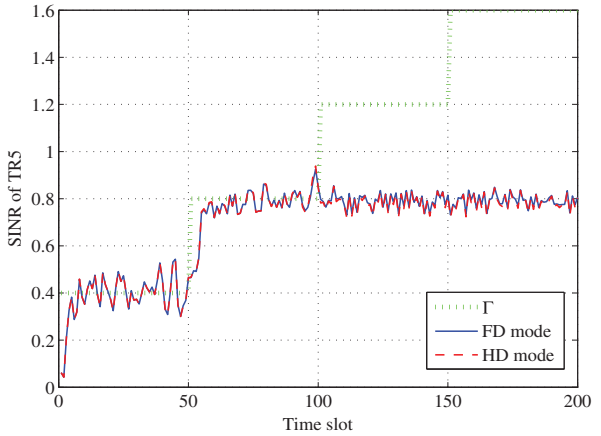

Fig. 14. Evolution of the SINR at TR_5 under varying Γ.

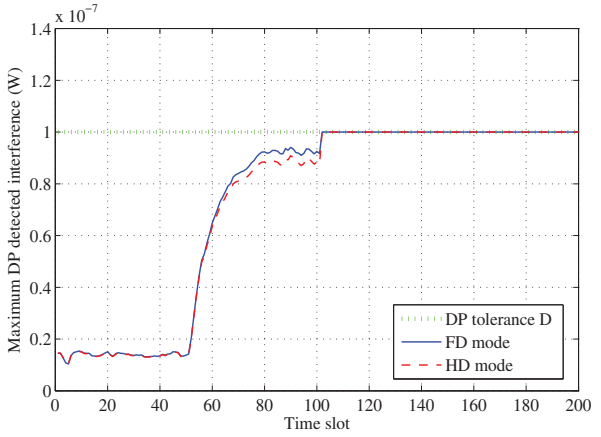

Fig. 15. Maximum measured interference among all the DPs under varying Γ.

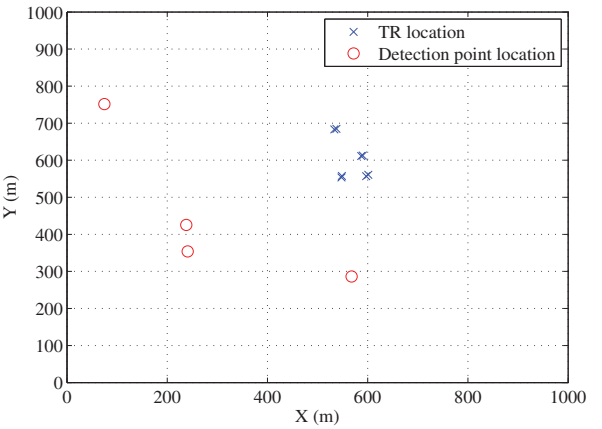

Fig. 16. Distribution of the TRs and DPs in the 1000 × 1000 m^2 network.

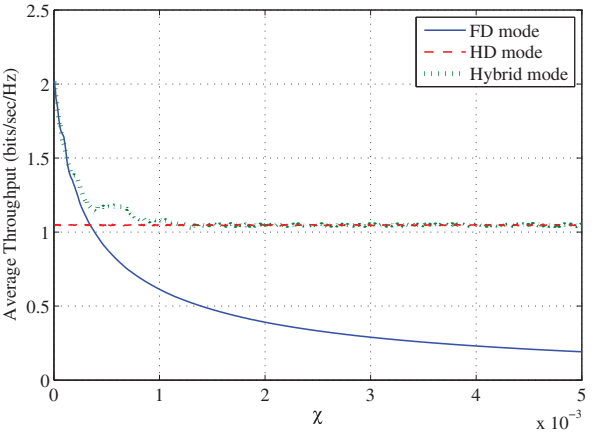

Fig. 17. Average throughput of the FD, HD, and hybrid modes for different values of χ.

with a $\Gamma \leq 0.8$, and the SINR of TR_5 can quickly follow Γ from 0.4 to 0.8. On the other hand, both SINR curves cannot follow the increased Γ beyond 0.8, because of a larger power is required to combat the residual self-interference in order to achieve the same SINR, which, however, is not allowed since the primary constraint of PU protection will be violated. In Fig. 15, the maximum measured interference among the DPs is also plotted. It can be seen that the primary goal of PU protection is always achieved by the proposed scheme when Γ is increased from 0.4 to 1.6 .

5.3. Throughput performance

In this section, we evaluate the achievable throughput by the proposed power control scheme. We focus on the proposed hybrid scheme in the simulations, with which the operating mode for each TR is determined as given in Section 4.2. The large 1000 × 1000 m^2 network with eight TRs and four DPs is used in the following simulations, as shown in Fig. 16.

In the simulation, we increase χ from 0.000005 to 0.005 with step size of 0.000005. With each χ value, we simulate the system for 200 time slots each with a random noise level, which has been shown to be sufficient long for convergence in our previous simulations. We plot the average throughput of the 200 time slots for each χ value in Fig. 17 for the FD, HD and hybrid schemes.

It can be seen in Fig. 17 that the hybrid scheme achieves the highest throughput for the entire range of χ. In particular, when $\chi \leq 3.43 \times 10^{-4}$, SIS is very effective and most of the TRs operate in the FD mode. The hybrid scheme achieves the same throughput as FD, which is higher than that of HD. As χ is increased, the advantage of FD transmissions diminishes and HD begins to achieve higher throughput than FD. When $3.43 \times 10^{-4} \leq \chi \leq 1.3 \times 10^{-3}$, some TRs operate in the FD mode and some others in the HD mode. When $\chi \geq 1.3 \times 10^{-3}$, all the TRs operate in the HD mode since the residual self-interference is so strong, there is no benefit for using FD transmissions. The proposed hybrid scheme compares the gains of FD and HD, and always chooses the better operating mode to achieve the highest throughput for the entire range of χ.

Finally, we investigate the impact of noise level. In the simulation, we set χ to 0.0005 and increase the noise power σ^2 from $10^{-6}W$ to $10^{-3}W$. The throughput results for the three schemes are presented in Fig. 18. As expected,

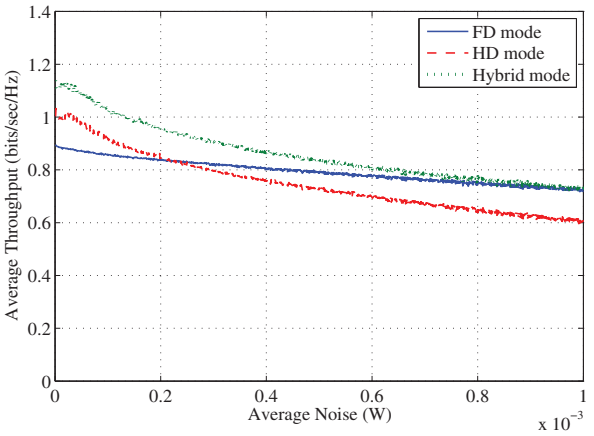

Fig. 18. Average throughput of the FD, HD, and hybrid modes for different values of σ^2.

the hybrid scheme achieves the highest throughput among the three, and the throughput decreases when noise is increased for all the three schemes. However, the influence of noise on throughput is different for the three schemes. As shown in (5), the FD mode has one extra interference source, i.e., the residual self-interference, making it less sensitive to the varying noise power. This is why the throughput of HD decreases faster than FD. The hybrid scheme can use FD instead of HD even though the χ value is larger in this simulation. The hybrid scheme always achieves the highest throughput in all the scenarios simulated.

5.4. Cellular FD CR network

The proposed mechanism can be adopted for other network scenarios. In this section, we consider an underlay CR network that coexists with a primary cellular network as described in a recent work [29], where joint power and admission control schemes are developed for the underlay cellular CR Network, which coexists with a primary cellular network with uplink transmissions.

We adopt a similar network scenario with the uplink transmissions of a primary cellular network that coexists with a number of FD SU links. In particularly, we simulate a 100 $\times$ 100 m^2 network with the PU BS, where the DP is located, right in the middle of the area at (50, 50). There are 8 pairs of SU devices that are randomly distributed in the are as shown in Fig. 19. Other parameters are set as $\Gamma = 0.8$; the noise power σ^2 is uniformly distributed in $[1.2 \times 10^{-7}, 2.4 \times 10^{-7}]$ W and the DPs' interference tolerance is set as $D_j = 1 \times 10^{-7}$ W for all j.

In Fig. 20, we present the simulation results on the network wide throughput for various χ values achieved by the HD, FD and hybrid transmission modes. Note that χ is in the log scale. It can be seen that, for the full range of achievable χ by the existing SIS cancellation techniques, the hybrid transmission mode achieves the highest total throughput among the three. FD is helpful when SIS is effect with a small χ; when χ is above 10^{-4}, FD does not perform as well as HD due to the large residual self-interference. The same trends are observed in this simulation as in the previous two scenarios.

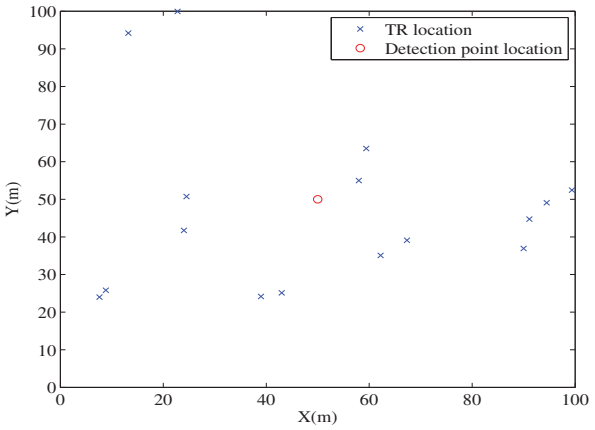

Fig. 19. Distribution of the TRs and the DP in the 100 $\times$ 100 m^2 network.

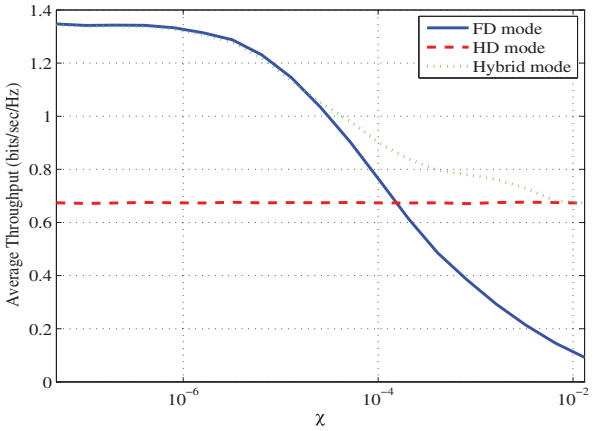

Fig. 20. Average throughput of the FD, HD, and hybrid modes for different values of χ with single DP.

6. Related work

FD transmission is a new technology to push the limit of single channel communications. In [7], the authors proposed basic concepts such as RF and digital cancellations and discusses potential MAC and network gains with full-duplexing. In [10], the authors presented the design and implementation of a real-time 64-subcarrier 10 MHz full-duplex OFDM physical layer, and demonstrated up to 80dB self-interference suppression with experiments. In [8], the authors presented a full duplex radio design using signal inversion and adaptive cancellation, as well as a full duplex MAC design and evaluation results with a testbed of 5 prototype FD nodes. In [9], a MIMO FD design was presented, while FD cellular networks have been investigated in some recent papers [30,31]. The achievable capacity gain of FD in a network setting is examined in a few recently works [12–14,38,39,40,41], where inter-link interference and spatial reuse are the major limiting factors for the FD gain [13].

CR has been recognized as an important technology for enhancing spectrum access efficiency [3,4]. In the class of overlay CR networks, SUs sense the spectrum and access the spectrum when PUs are absent. In the class of underlay CR networks, SUs coexist with PUs in the same spectrum

conditioned on limited interference to the PUs. Both techniques can be transparent to PUs [3]. In a recent work [11], the authors proposed to combine FD with CRs. The FD capability can be utilized to allow current two-way transmissions for the SUs, as well as enabling SUs to transmit while sensing.

There has been considerable work on power control and CU coexistence in underlay CR networks [29,32–35]. Most work has been focused on enabling underlay CR user transmissions while preserving the QoS of PU. In [32], a method is presented dedicated to DS-CDMA PU and OFDM SU networks exploiting PU power signaling, which targets at controlling the SU transmitting power while maximize SU transmission under slow shadowing and fast fading. Some other prior works focus on joint admission and power control [29,33], aiming to maximize the throughput by controlling the number of active SUs. In a recent work [34], power control for an underlay device to device network has been studied. The authors develop both centralized and distributed algorithms. In [35], power control in an FD network has also been studied, which is on power control for a single FD link. Few prior works consider power control for FD links in a network setting. To the best of our knowledge, our method is the first one to address the problem of power control in underlay FD CR networks with a control theoretic approach, and to deploy a distributed power control scheme for underlay FD CR networks.

Feedback control has found wide application in communication and networking systems. A modern overview of functionalists and tuning methods for PID controllers was presented in [27]. In [36], a proportional (P) controller was developed for streaming videos to stabilize the received video quality as well as the bottleneck link queue, for both homogeneous and heterogeneous video systems. In [26], the author presented a PID based power adjustment algorithm that was later extended in [5], which developed a PID control for power control in underlay CR networks. In [37], centralized and distributed algorithms are developed for downlink power control for streaming multiple variable bit rate (VBR) videos in a multicell wireless network.

7. Conclusion

In this paper, we investigated the design of effective power controllers for single channel underlay CR networks, where FD transmissions were exploited to improve network capacity. Taking the SIS factor into consideration, we investigated the design of a power control scheme that integrates a PID controller and a power constraint mechanism, and developed a hybrid FD–HD scheme to achieve the dual goals of PU protection and SU QoS provisioning. The stability performance of the proposed scheme was analyzed. The stability and throughput performance of the proposed schemes were validated with simulations.

Acknowledgment

This work is supported in part by the US National Science Foundation (NSF) under Grant CNS-0953513, the U.S. Naval Research Laboratory (NRL), and the Wireless Engineering Research and Education Center (WEREC) at Auburn University.

References

[1] N. Tang, S. Mao, S. Kompalla, Power control in full duplex underlay cognitive radio networks: a control theoretic approach, in: Proceedings of the IEEE MILCOM 2014, Baltimore, MA, 2014, pp. 949–954.
[2] Cisco Visual Networking Index (VNI), Feb. 2014, [Online]Available: http://www.cisco.com/.
[3] Q. Zhao, B.M. Sadler, A survey of dynamic spectrum access, IEEE Signal Process. Mag. 24 (3) (2007) 79–89.
[4] Y. Zhao, S. Mao, J. Neel, J.H. Reed, Performance evaluation of cognitive radios: metrics, utility functions, and methodologies, Proc. IEEE 97 (4) (2009) 642–659, doi:10.1109/JPROC.2009.2013017.
[5] G. Matsui, T. Tachibana, Y. Nakamura, K. Sugimoto, Distributed power adjustment based on control theory for cognitive radio networks, Elsevier Comput. Netw. 57 (17) (2013) 3344–3356.
[6] M. Duarte, A. Sabharwal, Full-duplex wireless communications using off-the-shelf radios: feasibility and first results, in: Proceedings of the ASILOMAR'10, Pacific Grove, CA, 2010, pp. 1558–1562.
[7] J.I. Choi, M. Jain, K. Srinivasan, P. Levis, S. Katti, Achieving single channel, full duplex wireless communication, in: Proceedings of the ACM MobiCom'10, Chichago, IL, 2010, pp. 1–12.
[8] M. Jain, J.I. Choi, T. Kim, D. Bharadia, S. Seth, K. Srinivasan, P. Levis, S. Katti, P. Sinha, Practical, real-time, full duplex wireless, in: Proceedings of the ACM MobiCom'11, Las Vegas, NV, 2011, pp. 301–312.
[9] E. Aryafar, M.A. Khojastepour, K. Sundaresan, S. Rangarajan, M. Chiang, MIDU: enabling MIMO full duplex, in: Proceedings of the ACM MobiCom'12, Istanbul, Turkey, 2012, pp. 257–268.
[10] A. Sahai, G. Patel, A. Sabharwal, Pushing the limits of full-duplex: design and real-time implementation, ArXiv preprint. arXiv:1107.0607.
[11] W. Afifi, M. Krunz, Exploiting self-interference suppression for improved spectrum awareness/efficiency in cognitive radio systems, in: Proceedings of the IEEE INFOCOM'13, Turin, Italy, 2013, pp. 1258–1266.
[12] Y. Yang, B. Chen, K. Srinivasan, N.B. Shroff, Characterizing the achievable throughput in wireless networks with two active RF chains, in: Proceedings of the IEEE INFOCOM 2014, Toronto, Canada, 2014, pp. 262–270.
[13] X. Xie, X. Zhang, Does full-duplex double the capacity of wireless networks, in: Proceedings of the IEEE INFOCOM 2014, Toronto, Canada, 2014, pp. 253–261.
[14] D.N. Nguyen, M. Krunz, S. Hanly, On the throughput of full duplex MIMO in the multi-link case, in: Proceedings of the WiOpt 2014, Hammamet, Tunisia, 2014.
[15] IEEE, July 2011, IEEE 802.22-2011(TM) Standard for Cognitive Wireless Regional Area Networks (RAN) for Operation in TV Bands.
[16] Y. Xu, S. Mao, Stackelberg game for cognitive radio networks with MIMO and distributed interference alignment, IEEE Trans. Veh. Technol. 63 (2) (2014) 879–892.
[17] N. Chatzidiamantis, E. Matskani, L. Georgiadis, I. Koutsopoulos, L. Tassiulas, Optimal primary-secondary user cooperation policies in cognitive radio networks, Dec. 2014, [online] Available: http://arxiv.org/abs/1307.5613. arXiv:1307.5613.
[18] S. Haykin, Cognitive radio: brain-empowered wireless communications, IEEE J. Sel. Areas Commun. 23 (2) (2005) 201–220.
[19] D. Hu, S. Mao, N. Billor, P. Agrawal, On the trade-off between energy efficiency and estimation error in compressive sensing, Elsevier Ad Hoc Netw. J. 11 (6) (2013) 1848–1857.
[20] J.M. Peha, Approaches to spectrum sharing, IEEE Commun. 43 (2) (2005) 10–12.
[21] S. Srinivasa, S.A. Jafar, Soft sensing and optimal power control for cognitive radio, in: Proceedings of the IEEE GLOBECOM 2007, Washington, DC, 2007, pp. 26–30.
[22] M.G. Khoshkholgh, K. Navaie, H. Yanikomeroglu, Impact of the primary network activity on the maximum achievable capacity of DS-CDMA/OFDM spectrum sharing, in: Proceedings of the IEEE VTC-Fall 2008, Calgary, BC, 2008, pp. 1–5.
[23] M.G. Khoshkholgh, K. Navaie, H. Yanikomeroglu, On the impact of primary network activity on the achievable capacity of spectrum sharing over fading channels, IEEE Trans. Wireless Commun. 8 (4) (2009) 2100–2111.
[24] K. Eswaran, M. Gastpar, K. Ramchandran, Cognitive radio through primary control feedback, IEEE J. Sel. Areas Commun. 29 (2) (2011) 384–393.
[25] S. Koskie, Z. Gajic, Optimal SIR-based power control strategies for wireless CDMA networks, J. Inform. And Syst. Sci. 1 (1) (2007) 1–18.
[26] F. Gunnarsson, F. Gustafsson, J. Blom, Pole placement design of power control algorithms, in: Proceedings of the IEEE VTC-Spring'99, Houston, TX, 1999, pp. 2149–2153.
[27] K.H. Ang, G. Chong, Y. Li, PID control system analysis, design, and technology, IEEE Trans. Control Syst. Technol. 13 (4) (2005) 559–576.

[28] ITURM, 1225, guidelines for evaluation of radio transmission technologies for IMT-2000, International Telecommunication Union.
[29] M. Monemi, M. Rasti, E. Hossain, On joint power and admission control in underlay cellular cognitive radio networks, IEEE Trans. Wireless Commun. 14 (1) (2015) 265–278.
[30] S. Goyal, P. Liu, S. Hua, S. Panwar, Analyzing a full-duplex cellular system, in: Proceedings of the CISS'13, Baltimore, MD, 2013, pp. 1–6.
[31] X. Shen, X. Cheng, L. Yang, M. Ma, B. Jiao, 2013, On the design of the scheduling algorithm for the full duplexing wireless cellular network, in: Proceedings of the IEEE Globecom'13, Atlanta, GA, pp. 1–6.
[32] M. Khoshkholgh, K. Navaie, H. Yanikomeroglu, Interference management in underlay spectrum sharing using indirect power control signalling, IEEE Trans. Wireless Commun. 12 (7) (2013) 3264–3277.
[33] I. Mitliagkas, N. Sidiropoulos, A. Swami, Joint power and admission control for ad-hoc and cognitive underlay networks: Convex approximation and distributed implementation, IEEE Trans. Wireless Commun. 10 (12) (2011) 4110–4121.
[34] N. Lee, X. Lin, J. Andrews, R. Heath, Power control for D2D underlaid cellular networks: Modeling, algorithms, and analysis, IEEE J. Sel. Areas Commun. 33 (1) (2015) 1–13.
[35] W. Cheng, X. Zhang, H. Zhang, Optimal dynamic power control for full-duplex bidirectional-channel based wireless networks, in: Proceedings of the IEEE INFOCOM'13, Turin, Italy, 2013, pp. 3120–3128.
[36] Y. Huang, S. Mao, S.F. Midkiff, A control-theoretic approach to rate control for streaming videos, IEEE Trans. Multimedia 11 (6) (2009) 1072–1081, doi:10.1109/TMM.2009.2026085.
[37] Y. Huang, S. Mao, Downlink power control for multi-user VBR video streaming in cellular networks, IEEE Trans. Multimedia 15 (8) (2013) 2137–2148, doi:10.1109/TMM.2013.2270457.
[38] M. Feng, S. Mao, T. Jiang, Joint duplex mode selection, channel allocation, and power control for full-duplex cognitive femtocell networks, Elsevier Digital Commun. Netw. 1 (1) (2015) 30–44.
[39] Z. Jiang, S. Mao, Online channel assignment, transmission scheduling, and transmission mode selection in multi-channel full-duplex wireless LANs, in: Proceedings of The 10th International Conference on Wireless Algorithms, Systems, and Applications (WASA 2015), Qufu, China, 2015, pp. 243–252.
[40] Y. Wang, S. Mao, Distributed power control in full duplex wireless networks, in: Proceedings of IEEE WCNC 2015, New Orleans, LA, 2015, pp. 1165–1170.
[41] M. Feng, S. Mao, T. Jiang, Duplex mode selection and channel allocation for full-duplex cognitive femtocell networks, in: Proceedings of IEEE WCNC 2015, New Orleans, LA, 2015, pp. 1900–1905.

Ningkai Tang received the M.S. degree in Electrical & Computer Engineering from Auburn University, Auburn, AL and the B.E. degree in Information science & engineering from Southeast University, Nanjing, China in 2014 and 2010, respectively. Since Spring 2015, he has been pursuing the Ph.D. degree in the Department of Electrical and Computer Engineering, Auburn University, Auburn, AL. His research interests include Cognitive radios, Full-duplex transmissions, smart grid, machine learning, and control theory.

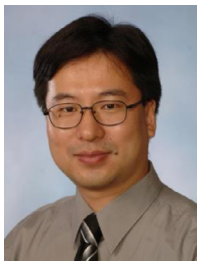

Shiwen Mao received Ph.D. in electrical and computer engineering from Polytechnic University, Brooklyn, NY. Currently, he is the Samuel Ginn Endowed Professor and Director of the Wireless Engineering Research and Education Center (WEREC) in the Samuel Ginn College of Engineering, Auburn University, Auburn, AL, USA. His research interests include wireless networks and multimedia communications, with current focus on cognitive radio, small cells, mmWave networks, free space optical networks, and smart grid. He is a Distinguished Lecturer of the IEEE Vehicular Technology Society in the Class of 2014. He is on the Editorial Board of IEEE Transactions on Multimedia, IEEE Internet of Things Journal, IEEE Communications Surveys and Tutorials, IEEE Multimedia Magazine, Elsevier Ad Hoc Networks Journal, among others. He is the Vice Chair-Letters & Member Communications of IEEE ComSoc Multimedia Communications Technical Committee. He received the 2013 IEEE ComSoc MMTC Outstanding Leadership Award and the NSF CAREER Award in 2010. He is a co-recipient of the IEEE WCNC 2015 Best Paper Award, the IEEE ICC 2013 Best Paper Award, and the 2004 IEEE Communications Society Leonard G. Abraham Prize in the Field of Communications Systems.

Sastry Kompella received the B.E. degree in Electronics and Communication Engineering from Andhra University, India, in 1996, the M.S. degree in Electrical Engineering from Texas Tech University, in 1998, and the Ph.D. degree in Electrical and Computer Engineering from the Virginia Polytechnic Institute and State University, in 2006. Currently, he is the Head for the wireless network research section under the Information Technology Division, U.S. Naval Research Laboratory, Washington, DC. His research interests include various aspects of wireless networks, from mobile ad hoc to underwater acoustic networks, with specific focus toward the development of cognitive and cooperative netwsork optimization techniques for efficient wireless link scheduling.